

COMPUTATIONAL AND EXPERIMENTAL INVESTIGATION OF CATHODIC PROTECTION DISTRIBUTION IN REINFORCED CONCRETE MARINE PILING

S.C. Kranc⁺, Alberto A. Sagüés⁺ and Francisco J. Presuel-Moreno⁺⁺
Department of Civil and Environmental Engineering
College of Engineering
University of South Florida
Tampa, FL, 33620

ABSTRACT

A detailed computer model of corrosion distribution in reinforced concrete has been used to predict the extent of cathodic protection provided for partially submerged piles by a combination of bulk sacrificial anodes placed below water and surface anodes above water. The model predictions are directly compared with the experimental response to cathodic protection in laboratory piles having active corrosion in progress.

INTRODUCTION

Chloride penetration of the concrete cover is a leading cause of significant corrosion damage in steel reinforced concrete marine structures. It is possible however, to intervene in this deterioration by the installation of cathodic protection systems. The goal of the present paper is to introduce a quantitative model to analyze the effectiveness of cathodic protection in marine piling by combining bulk and surface anodes. This investigation involves initial model calibration by comparison between results obtained in a laboratory investigation of small scale pilings and a computer generated model. Ultimately, it is hoped that a study of this nature will lead to improved techniques of application of cathodic protection, based on initial field data and a predictive model.

Keywords: Concrete, corrosion, reinforcing, cathodic protection

⁺ Professor

⁺⁺ Research Assistant, Permanent Affiliation: CINVESTAV-Mérida, México

Copyright

©1997 by NACE International. Requests for permission to publish this manuscript in any form, in part or in whole must be made in writing to NACE International, Conferences Division, P.O. Box 218340, Houston, Texas 77218-8340. The material presented and the views expressed in this paper are solely those of the author(s) and are not necessarily endorsed by the Association. Printed in the U.S.A.

EXPERIMENTAL PROCEDURE

The laboratory test specimens consisted of reinforced concrete columns 244 cm (96 in) high, with a square cross-section 12.7 cm (5 in) on the side. The concrete composition of the column had a water/cementitious ratio of 0.45. The total cementitious content was 302 Kg/m³ (512 pounds per cubic yard (pcy)). The mix had Portland cement Type II and Fly Ash class F in an amount equal to 20% of the total cementitious weight. (The rest of the mix design specifications can be found in ¹). Each column contained two No. 4 (1.27 cm diameter) rebars placed lengthwise at corners of the cross section diagonally opposite one another. The concrete cover was 2.5 cm (1 in.). These rebars were designated "A" and "B" for identification purposes. Each rebar was cut into four separate segments that were 57 cm (22.5 in) long, in order to permit testing at four elevations, as shown in Figure 1. Each segment was provided with an individual electric connection to a switch box on the outside of the column and normally the segments of each rebar were kept electrically connected to each other. Initially the two rebars were electrically separated, but they were interconnected and allowed to mutually stabilize for two weeks before application of the cathodic protection anodes. Four solid reference electrodes (activated titanium²) were positioned in the center line of the column at the midpoint of each rebar-segment. The electrodes were connected by wires to an external contact box and calibrated periodically against a saturated Calomel electrode (SCE).

The columns were placed in a fiberglass tank containing 5% NaCl water solution. The lower 63 cm (~25 in) of each specimen was submerged, with the lower rebar segment (Level 4) completely under the water line, while the remaining segments were completely above water. The surface of the concrete extending from the water line to 63 cm (25 in) above it (Level 3), was splashed with the salt-water solution, by means of a hose and pump, five times a week. This portion of each column simulated a region termed the "splash-evaporation zone", present in actual field service. The potential of the rebars, the macrocell currents and the resistance between rebars at the different levels for the rebar were monitored regularly.

Two of the test columns were selected for detailed examination. The results from both columns were comparable. The specific results for one of those columns (Column No. 4) are given in this paper. After nearly five years of exposure the column exhibited a crack along one of the rebars (Rebar B). The crack started ~25 cm (10 in) above the water line and was approximately 1 mm wide and 20 cm long. The crack was observed on both concrete surfaces adjacent to the rebar. The rebar A developed a rusted spot 3 cm long ~3 cm above the water line, suggesting localized corrosion at this level.

Application of Cathodic Protection

A principal part of the experiments reported here involves the installation of a sacrificial anode system using a zinc alloy and bulk anode materials comparable with those used in the field by the Florida Department of Transportation³. The zinc bulk anode was employed primarily to protect the section below water and a zinc mesh was installed to form a surface anode as depicted in Figure 1 for the splash zone. Four zinc mesh pieces of 12.7 cm (5 in) by 53 cm (21 in) were interconnected by means of 10 gage copper wire. The effective length of the anode is 50 cm (20 in). The 10 cm (4 in) immediately above the water line were not covered with the surface anode. The surface anode assembly consisted of cloth sponge placed next to the concrete surface, then on top of the sponge the zinc mesh was placed and covered with a plastic grid. The arrangement was held together with clamps at three different levels. The surface anode was installed and left in place for one week but not connected to the structure. During this period the splash zone was wetted once a day, as before. The surface anode was then connected to the structure. The bulk anode was connected to the structure five days later. The

system was allowed to stabilize for 40 days afterwards before obtaining the measurements described here.

Computer Model

The computer model used in the present investigation is a variation of a three dimensional, finite difference scheme presented in detail in references^{4,5}, so a detailed description will not be repeated here. The dimensions of the model correspond to the laboratory scale models described above having 192 nodes in the vertical dimension and 13 by 13 nodes in the horizontal plane. This node spacing corresponds to a grid spacing 1 cm in the horizontal and 1.25 cm in the vertical direction.

The concrete is treated in the computer model as having variable electric resistivity, ρ , and oxygen diffusivity, D but otherwise as a homogeneous medium. For this case, the governing equations for the diffusion of oxygen and the electrical potential (assuming charge neutrality) in the electrolyte volume are $\nabla(D(\nabla C))=0$ and $\nabla(\rho^{-1}(\nabla E))$.

Conventional boundary conditions at the external surfaces specify either the field quantity (potential, E or oxygen concentration, C) or fluxes of oxygen and electric charge. The program structure permits the introduction of experimental or hypothetical variation in oxygen diffusivity and concrete electrical resistivity with elevation as well as boundary conditions at the external surface. The values used in the computer model were chosen to be similar to the measured values. For the level below water and above the splash zone two constant resistivity values were used. The resistivity of the splash zone was assumed to increase exponentially with elevation before anode application, and considered as a constant value afterwards. The values assumed for oxygen diffusivity and resistivity are identified in Figure 2, and shown in Table 1.

Boundary conditions at the reinforcing steel are formulated from the electrochemical reactions taking place on the surface. In the present study, it is assumed that surface reactions are governed by Butler-Volmer kinetics. At active steel surfaces, both oxygen and iron dissolution are considered to be governed by Butler-Volmer kinetics. At passive rebar surfaces, oxygen reduction is also assumed to take place and is governed by Butler-Volmer kinetics. However, the iron dissolution in the passive rebar surfaces is assumed to proceed at a small and constant rate typical of passive steel and does not obey the Butler-Volmer kinetics. Reverse reactions, which can often be neglected in the problems of practical interest⁶, were considered non-existing in the computer model.

Applying Ohm's law locally, the normal gradient of the potential at the surface is proportional to the sum of all current densities(i), $i=\rho^{-1}\nabla E$. Likewise, the equivalent current density due to the consumption of oxygen is given by Fick's first law by $i_c = 4FD(\nabla C)$ (i_c is the cathodic current), which is the boundary condition for the consumption of oxygen at the steel surface. The factor 4 appears as the number of electrons transferred in the reduction reaction, and F is Faraday's constant.

Provision was made for the presence of the hydrogen evolution reaction. The reverse reaction is neglected. The model is sufficiently detailed to yield local predictions of oxygen concentration, potentials and currents everywhere in the concrete, as well as along the steel concrete interface. Most importantly, the macrocell currents in the rebar segments corresponding to the experimental model as well as the potentials on the external surface can be calculated directly.

Several modifications were incorporated into the program to simulate the action of the bulk and surface anode. The operating potentials of both anodes were nearly -1000 mV vs. SCE. For the bulk anode an equipotential value of -1000mV vs. SCE was therefore imposed on the surface of the concrete below water. In a similar manner the potential at the concrete surface covered by the anode at the splash zone was set at -1000mV vs. SCE. Experimentally it was found that after a few days following placement of the surface anode assembly the resistivity of the concrete at the splash zone level decreased significantly due to water uptake. The resistivity actually decreased to a value smaller than that observed below water, probably due to a higher Cl concentration (after years of salting) in the splash zone than below water. Thus to model the protective condition, the resistivity profile was changed to reflect the new conditions as shown in Figure 2. For the level below water and above the splash zone the value was considered constant and equal to that encountered before anode placement. The diffusivity for the splash zone after protection was assumed to be reduced also due to the concrete becoming more nearly saturated as opposed to that before placing the surface anode.

In the computer model, the steel was considered fully active below water in both rebars. Based on the potential and cracking patterns observed at the splash zone (Level 3), the active zone of rebar A was assumed to extend to 2.5 cm (1 in) immediately above the water line. The rebar B was considered to have a 15 cm (6 in) long active steel segment above water, ending 3.75 cm (1.5 in) from the top of the splash zone. The remaining portion of both rebars were considered passive.

RESULTS AND DISCUSSION

Observations made before protection was installed

Surface potential profile measurements were made after the rebars were interconnected for ~ 1 week, when the system was still in a freely corroding state. The potential at the surface of the concrete along the rebar was measured directly over each rebar, as shown in Figure 3. The values are the average of four days. Potential measurements based on the embedded reference electrodes are shown for other concrete zones. Attempts to predict the potential profile by proposing the active-passive zone distribution shown in Figure 2 were relatively successful as indicated by the similarity between potential model and experimental trends in Figure 3. Differences between prediction and actual measurements could be further diminished by refining the choice of parameters in Table 1, especially those for transport of oxygen, and the resistivity profile.

The second observation involved macrocell currents measured across the three points along each rebar identified in Figure 1, compared again to the predictions of the numerical model. The comparison was made using the net macrocell current produced or consumed by each rebar element (obtained by difference from those measured at the test points). The averages of 4 days are shown in Table 2. The measured currents confirm that the elements below water are net anodes. The rebars in the splash zone were net cathodes. The upper two zones showed much less electrochemical activity. Rebar A was delivering a modest net electronic flow of ~ 31 μA to rebar B. The model computations gave also a small current (~ 12 μA) in the same direction for the net electronic flow. The modelled and the measured currents at the different rebar elements have the same sign and comparable values. Trial calculations showed that the net current values, while remaining of roughly the same magnitude, were quite sensitive to the exact choice of active-passive spatial distribution in Level 3. In the absence of detailed information on the precise corrosion distribution in that zone, the assumed distribution was left as shown in Figure 2, which was chosen based on the externally measured potential and cracking profile.

The parameters that resulted in the best approximation are displayed in Table 1. It was found that the distribution of electrochemical action that best represents the laboratory rebars has the following characteristics; i) below water the rate of the anodic reaction is greater in rebar A than in rebar B. This was implemented in the model by assuming a correspondingly greater effective value of i_0 for iron oxidation. ii) at the crack level of rebar B the rate of the anodic reaction for a given potential appeared to be significantly greater than elsewhere. Therefore, i_0 was taken to be a factor of ten greater than that below water. This increased anodic action is possibly due a higher Cl^- concentration at the splash zone, and the wet conditions present at the crack.

Observations following the application of cathodic protection

It was observed that the installation of the wet anode assembly caused a substantial reduction in the resistivity at the mid level of the column, as seen in Table 3. This effect is likely due to the increased moisture in the concrete covered by the surface anode and the wet sponge. The values in Table 3 are based on resistance measurements between rebars and converted to resistivity by using the average resistance and the cell constant. These values were the base for the ones used in the model (Table 1 and Figure 2). In the computer model a value of 500 k Ω -cm was considered for levels 1 and 2, before and after protection. Only negligible variations resulted from increasing in the model the 500 k Ω -cm value used in level 4.

After the first week following anode placement, the surface anode was connected to the rebar and five days later the bulk anode was connected. After approximately 45 days with both anodes, the currents provided by the anodes were considered stable. Table 4 shows the values of the net currents for the model and for the laboratory measurements. The experimental values were obtained by averaging five measurements made at different days.

Level 3 received most of the protective current, followed by levels 4, 2 and 1. This behavior was replicated by the model calculations, which provided reasonable quantitative agreement when considering the average current for each level. The model predicts a moderate amount of hydrogen evolution ($\sim 1 \mu\text{A}/\text{cm}^2$) at level 4. The surface anode delivered a protective current that was several times greater than that of the bulk anode, an observation also replicated by the model calculations (Tables 4 and 5).

After 50 days from anode placement, the potential was mapped over the concrete surface of the splash zone not covered with the surface anode. Potential was also measured in the region 12.5 cm (5 in.) immediately above the surface anode. The potential below the water predicted by the model, at the rebar surface was approximately 65 mV more positive than at the concrete surface. Figure 4 depicts the potential distribution with protection installed, compared to model predictions. The effect of protection is clearly evident and the model predictions showed reasonable agreement with these results.

CONCLUSIONS

1. An experimental investigation of a cathodic protection scheme involving both surface anodes and bulk anodes has been conducted under laboratory conditions. The results agree with the general behavior expected from a partially submerged column under cathodic protection.
2. Utilizing a detailed computer model developed previously it was possible to make reasonable predictions of the freely corroding state. Modification of the program to include the action of the cathodic protection scheme permitted prediction of the amount of current required by the structure and the potential distribution under protective conditions.

ACKNOWLEDGEMENT

This work was partially supported by the Florida Department of Transportation (FDOT), and Engineering Computing Services of the University of South Florida (USF). The opinions, findings and conclusions expressed here are those of the authors and not necessarily those of any sponsor. One of the authors (F.P-M.) acknowledges the scholarship provided by the National Council of Science and Technology (CONACYT-México).

REFERENCES

1. Alberto A Sagüés, "Factors Controlling Corrosion of Steel-Reinforced Concrete Substructure in Seawater", Final Report to Florida D.O.T., WPI No. 0510537, University of South Florida, Tampa, 1994
2. P. Castro, A. Sagüés, E. Moreno, L. Maldonado, L. Genescá, *Corrosion*, 52, 8(1996): p. 609.
3. R.J. Kessler, R.G. Powers and I.R. Lasa, "Zinc mesh anodes cast into concrete pile jackets", *Corrosion'96*, paper no 327 (Houston, TX: NACE, 1996).
4. S.C. Kranc, Alberto A. Sagüés, "Modelling the distribution of corrosion on reinforcing steel in concrete", in the Proceedings of the IASTED/ISMM International conference Modelling and Simulation held in Pittsburgh, Pennsylvania, USA, April 1995
5. Alberto A Sagüés, S. C. Kranc and B. G. Washington, "Computer Modelling of Corrosion and Corrosion Protection of Steel in Concrete", in *Concrete 2000*, eds. R.K. Dhir and M.R. Jones, (London, UK, Chapman & Hall, 1993): p. 1275
6. H. Uhlig and R. Revie, *Corrosion and Corrosion Control*, 3rd ed., (New York, NY: John Wiley, 1985)

Table 1. Model Parameters

- Concrete Resistivity and Oxygen Diffusion Coefficient (Keyed to Figure 2)

	Resistivity (kΩ-cm)			Oxygen Diffusion Coefficient D (cm ² /s)		
	ρ_L	ρ_M	ρ_H	D_L	D_M	D_H
Before Anode Placement (B)	35	90	500	6×10^{-6}	6×10^{-4}	6×10^{-4}
After Anode Placement (A)	35	22	500	6×10^{-6}	9×10^{-5}	6×10^{-4}

- The resistivity profile and diffusivity profiles are shown in Figure 2. These parameters are derived from experimental data and the literature
- The concentration of O₂ at concrete surface is 3×10^{-7} moles/cm³
- The effective concentration of O₂ is expressed in moles of O₂ per cm³ of pore water in concrete. The values of the diffusivity selected reflect that choice of concentration units.
- Kinetic Parameters (Note that only forward reactions are being considered)

Reaction	i_o (μ A/cm ²)	E° (mV) (SCE)	β (mV/decade)
Oxygen Reduction	3×10^{-2}	- 20	160
Hydrogen Evolution	3	- 1000	120
Fe Dissolution (active steel bar A)	2×10^{-7}	- 920	60
Fe Dissolution (active steel bar B, BW*)	1×10^{-7}	-920	60
Fe Dissolution (active steel bar B, Crack)	2×10^{-6}	- 920	60
Fe Dissolution (passive steel bar A,B **)	0.03		

* BW= Below Water,

** In Passive Steel (Fe Dissolution has no Butler-Volmer dependence)

Table 2. Net electronic current (μA) leaving (+) or sinking in (-) each rebar element before CP installation

	Rebar A		Rebar B	
	Model	Laboratory	Model	Laboratory
Level 4	98	169	46	42
Level 3	-82	-132	-53	-63
Level 2	-4	-5	-5	-10
Level 1	~0	0*	~0	0*
Balance	12	31	-12	-31

*Estimated

Table 3. Effect of installation of protection on concrete Resistivity ($\text{k}\Omega\text{-cm}$)

	Before placing anodes	With anodes in place
Level 4	35	35
Level 3	90	18
Level 2	540	380
Level 1	1300	1300

Table 4. Net electronic current (μA) leaving (+) or sinking (-) each rebar element after CP installation

	Rebar A		Rebar B	
	Model	Experimental	Model	Experimental
Level 4	-324	-305	-324	-224
Level 3	-1737	-2552	-1739	-1250
Level 2	-196	-113	-196	-112
Level 1	~0	23	~0	0

Table 5. Net current delivery by anodes, comparison between model prediction and experimental observations(μA).

	Model	Experimental
Bulk Anode	779	470
Surface Anode	3737	4063

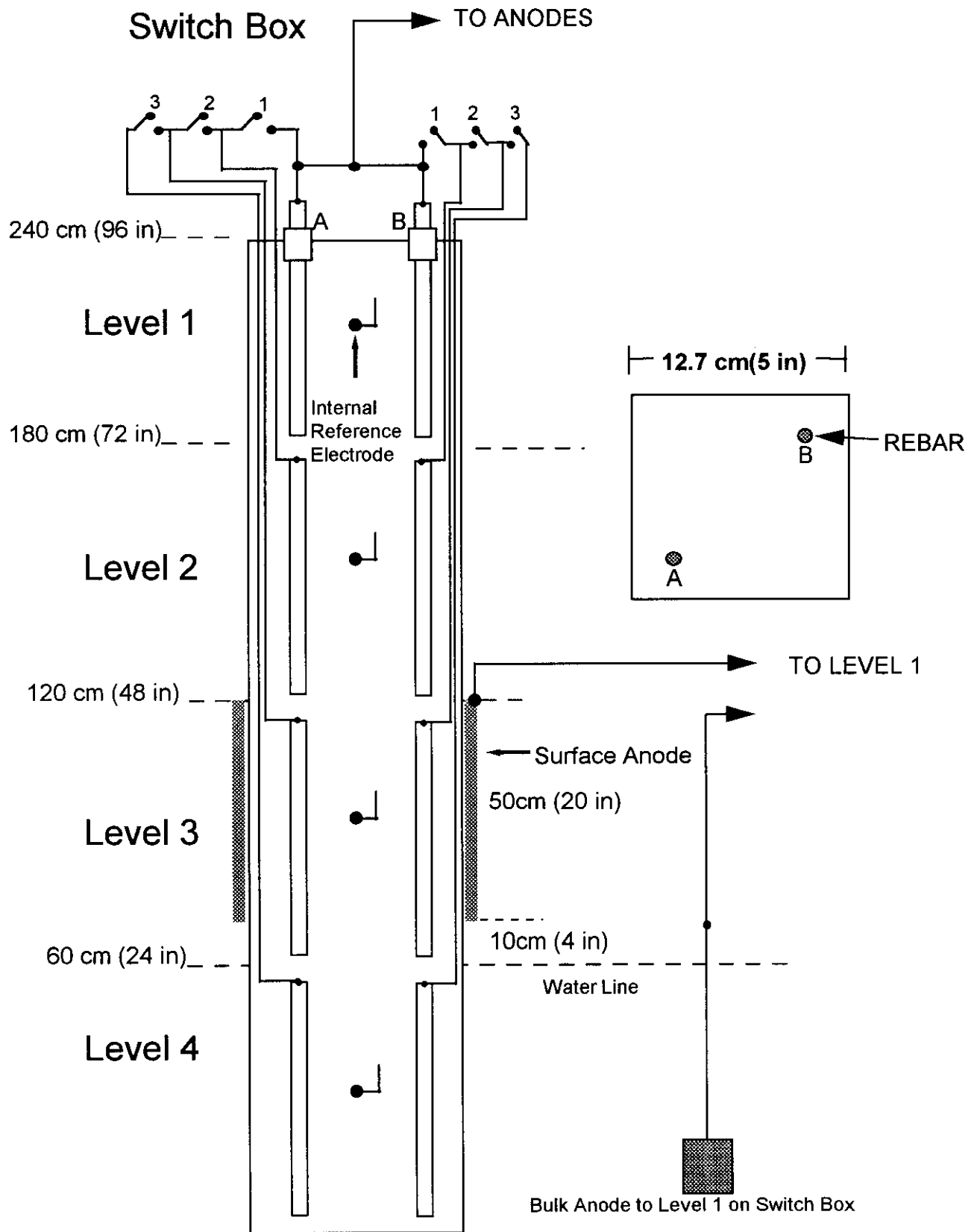


Figure 1. Experimental System Diagram

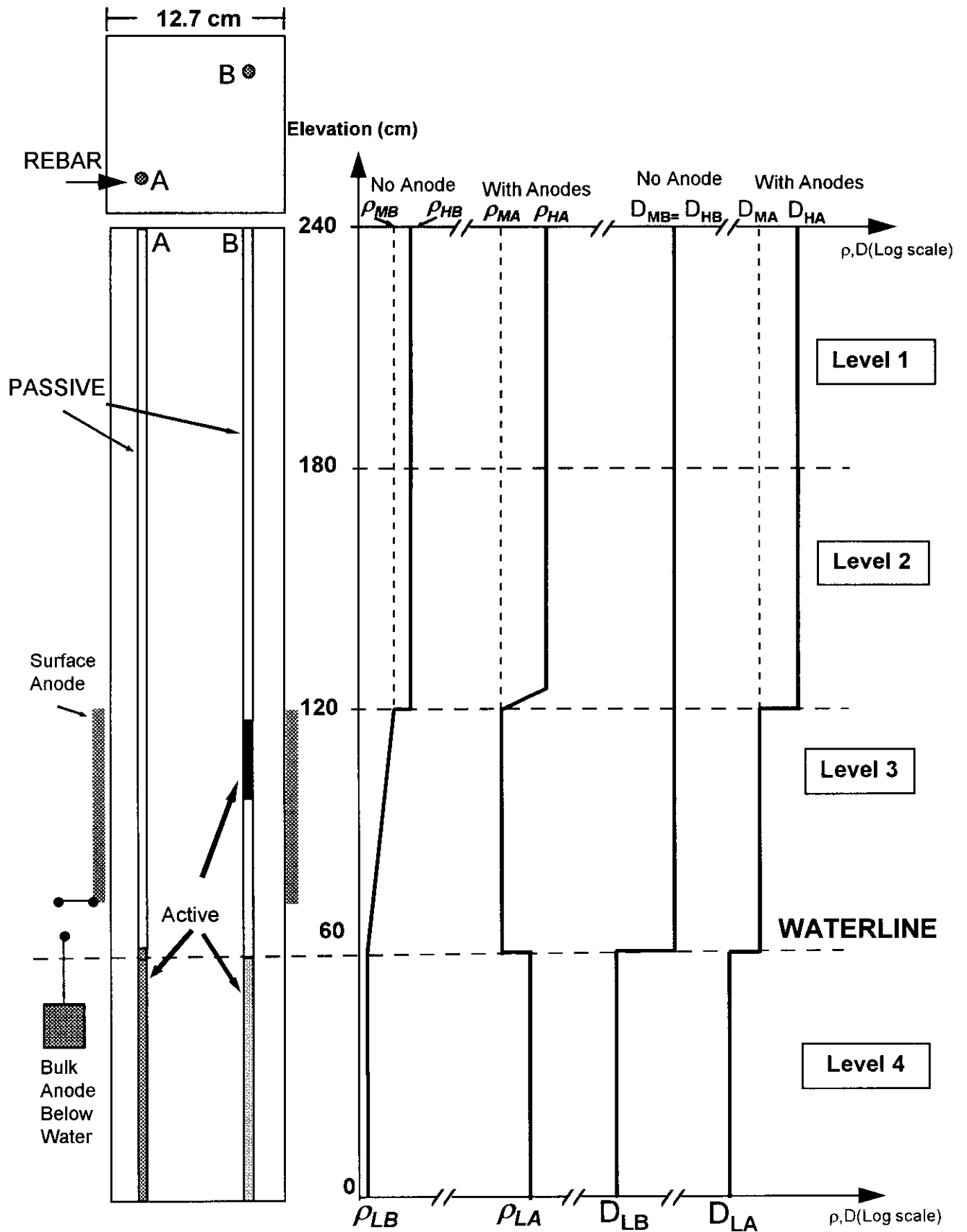


Figure 2. Model System Diagram

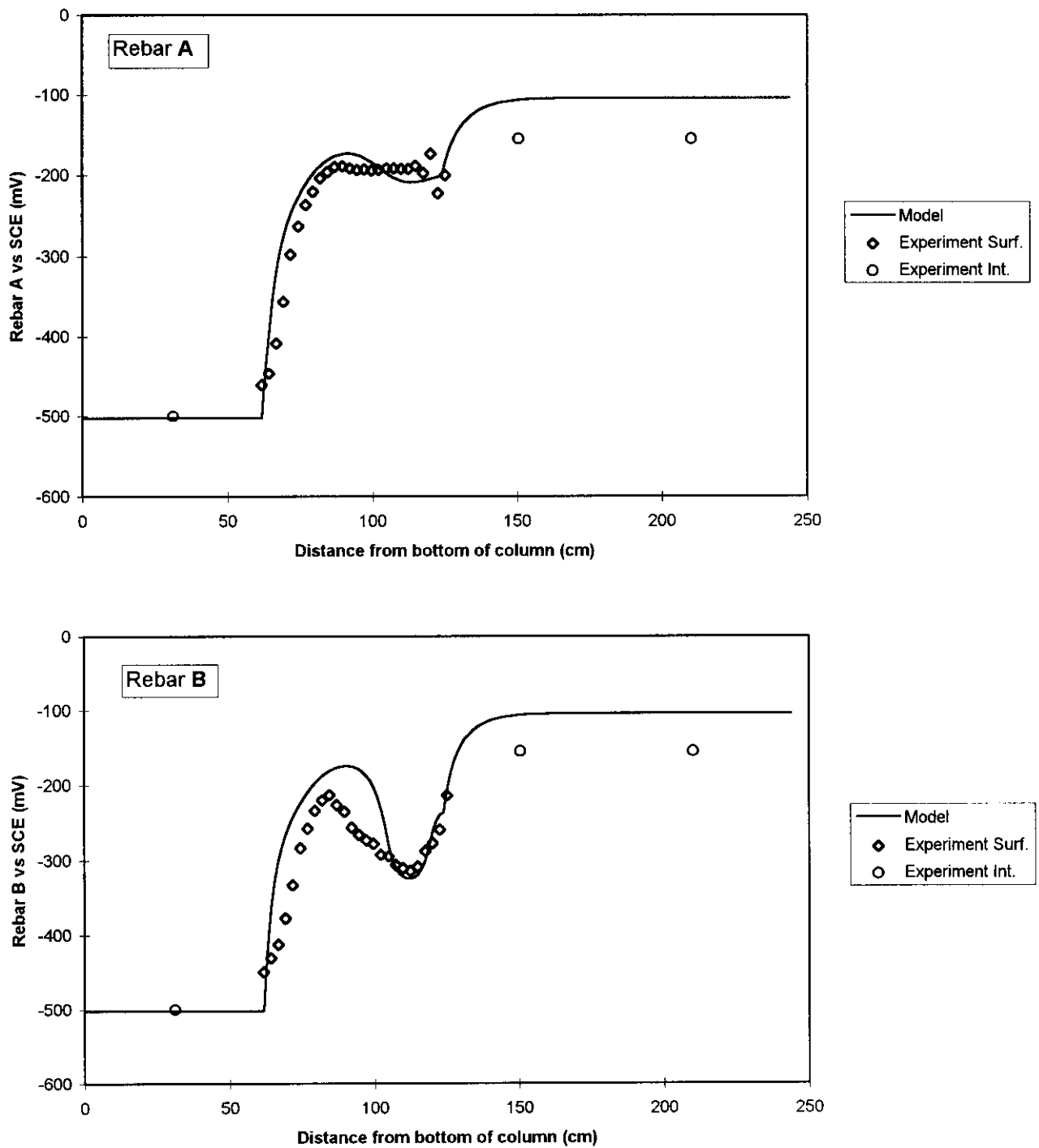


Figure 3. Potentials at the concrete surface along each rebar. (The open circles correspond to internal potentials measured using the embedded reference electrodes). Each experimental surface potential is the average of 4 measurements after interconnection.

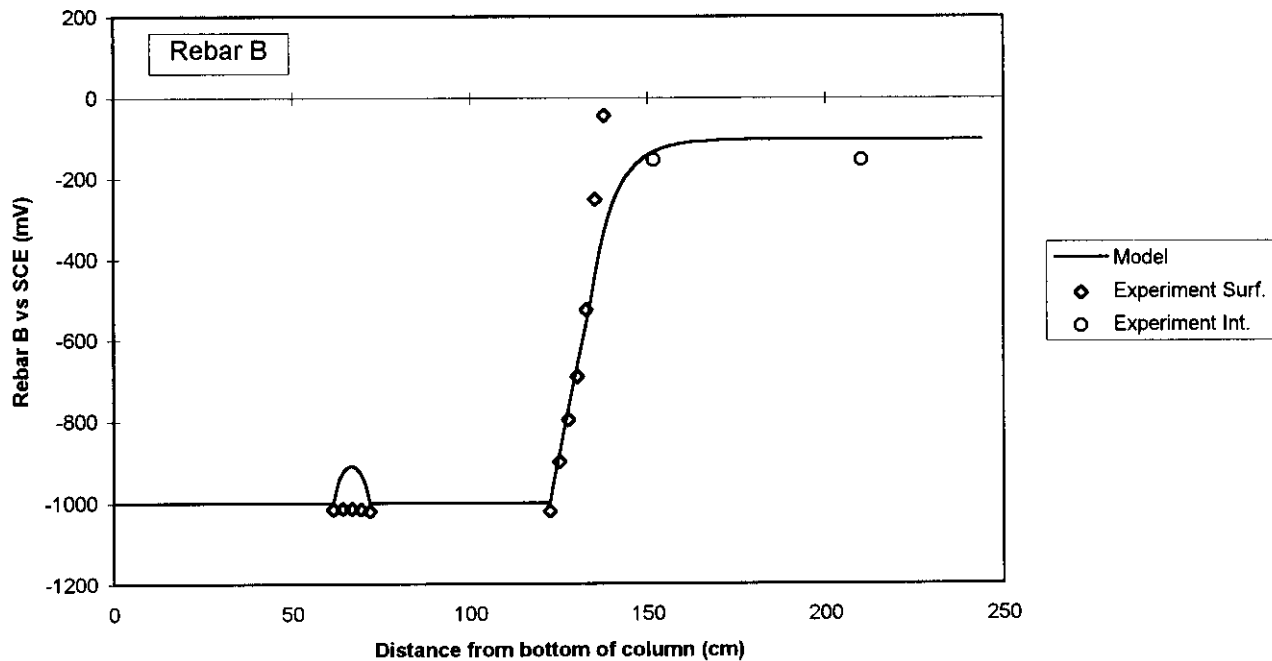
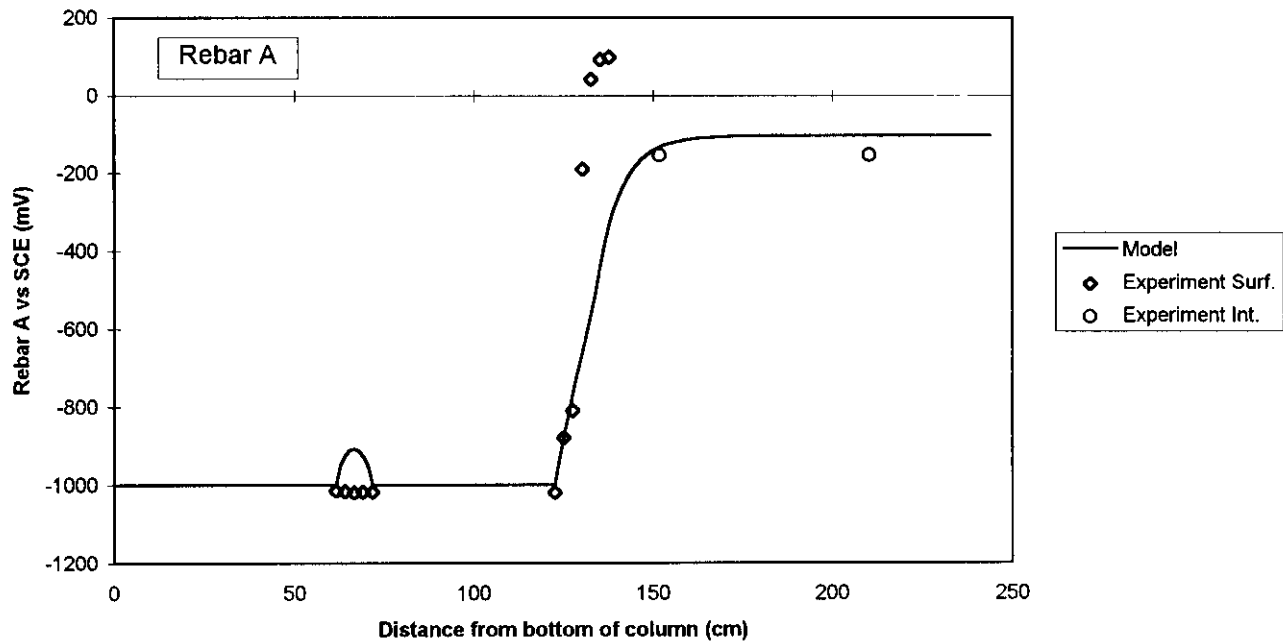


Figure 4. Potential at the concrete surface along each rebar. (The open circles correspond to internal potentials measured using the embedded reference electrodes) The experimental surface potentials were taken with both the bulk and the submerged anodes in place.